Newtonian Labs Teaching Guides
- The Physics of Electrodynamic Ion Traps -

Table of Contents

1 Introduction **1**

1.1 Earnshaw's Theorem 2

1.2 Ion Trapping Physics 2

2 Basic Trap Dynamics **2**

2.1 A Uniform Field Example 2

2.2 Add an Electric Field Gradient 3

3 Quadrupole Traps **5**

4 The Triboelectric Series **8**

5 Damped Ion Traps **8**

5.1 Stokes Damping 10

5.2 Particle Dynamics in a Quadrupole Trap 11

6 Extended Orbits **13**

6.1 The Ring Trap 13

6.2 The Linear Trap 14

1 Introduction

The purpose of this *Teaching Guide* is to examine the physics behind electrodynamic ion traps, and specifically to take a close look at the Newtonian Labs *Electrodynamic Ion Traps* (EIT) apparatus. Electrodynamic ion traps, also known as *Paul traps*, provide a means to guide the motion of charged particles, especially confining charged particles in free space using only time-varying electric fields. Wolfgang Paul and Hans Dehmelt received the Nobel Prize for Physics in 1989 for developing ion traps, and this technology is still in widespread use today.

Electrodynamic Paul traps operating at MHz frequencies can hold individual atomic or molecular ions, and these traps are commonly used as starting points for physics experiments investigating atomic or molecular properties. Paul traps have been used for building rudimentary quantum computers as well, in which the individual ions serve as qubits that can be examined using probe lasers. Ion trapping techniques are also commonly used in chemical mass spectroscopy, for determining the molecular weights of complex compounds with high precision.

Our focus below will be on trapping larger particles – about 25 μm in diameter – using electric fields oscillating at 60 Hz. The ion traps themselves are a few centimeters in size, operating in air, and the particles are illuminated using laser light, making them easily visible to the naked eye. Additional information about the EIT apparatus can be found in our *Instrument Description* document. In addition, several experiments that can be done using this hardware are described in our *Guide to Experiments* document. Both documents are available online at *NewtonianLabs.com*.

1.1 Earnshaw's Theorem

The basic idea of an ion trap is to confine a charged particle in free space, away from any other matter, using electric fields alone. There is a famous theorem, called *Earnshaw's theorem*, stating that one cannot construct a stable ion trap using electrostatic fields alone. To trap a positively charged particle at some position in space, for example, the electric field vectors around that position would all have to be pointing inward. And Maxwell's equations, specifically Gauss's Law, tell us that this is impossible unless there is a net negative charge at that position. So, try as one might, fundamental laws of physics tell us that it is not possible to create a static electric field geometry that will stably trap charged particles in free space.

There are magnetic variations of Earnshaw's theorem as well, for example stating that you cannot stably trap a bar magnet in free space using only static magnetic fields. Adding gravity does not help, and another version of Earnshaw's theorem states that you cannot levitate a stationary permanent magnet using only static magnetic fields.

Fortunately, there are many routes around Earnshaw's theorem. One popular engineering method is to use active feedback. For the magnetic case, one can continually measure the position of a levitated magnet and adjust the forces appropriately to keep the magnet positioned where you want it. This method is relatively cheap and easy to implement, and magnetically levitated trains work this way. Another way around Earnshaw's theorem for magnetic levitation is to use a spinning magnet instead of a stationary one. There is a toy called the *Levitron* (easily found online) that demonstrates levitation of a spinning magnet without using active feedback.

Paul and Dehmelt got around Earnshaw's theorem by using oscillating electric fields, since the theorem strictly applies only to static fields. It is not immediately obvious that you can use oscillating fields to trap particles (hence the Nobel Prize), so our first task is to understand the basic physics behind all this.

1.2 Ion Trapping Physics

Our goal in this document is to write down a fairly detailed description of the physics of electrodynamic ion trapping, with our main focus being on the EIT instrument. Thus our description will apply to the 25-micron-diameter particles used in the EIT experiment, trapped in air using high-voltage 60-Hz electric fields. This document is meant for the instructor and more advanced students, so it includes a fairly mathematical treatment of the subject. Furthermore we will examine some of the more subtle aspects of this experiment, for example the extended orbits described below. For a mathematics free (almost) explanation of ion trapping, more suitable for beginning physics students, please see our *Physics of electrodynamic ion traps - A qualitative description*, available at NewtonianLabs.com.

2 Basic Trap Dynamics

2.1 A Uniform Field Example

To begin, consider a charged particle placed inside an ideal parallel-plate capacitor, as shown schematically in Figure 1. Assume that the plates are large and separated by a distance d, and there is a vacuum between the plates. As long as the fields do not change too rapidly, we can assume a uniform electric field in the space between the plates, at any time equal to $E(t) = V(t)/d$, where $V(t)$ is the applied voltage. Assume a sinusoidally oscillating voltage, $V(t) = V_0 \cos \omega t$, which gives an electric field between the plates $E(t) = E_0 \cos \omega t$, with $E_0 = V_0/d$. In this field we place a particle having a charge q, as shown in the Figure.

The time-dependent electric force on the particle is $F(t) = qE(t) = qE_0 \cos \omega t$, so the motion of the particle in the z direction is described by the equation of motion $(F = ma)$

$$m\ddot{z} = qE_0 \cos \omega t$$

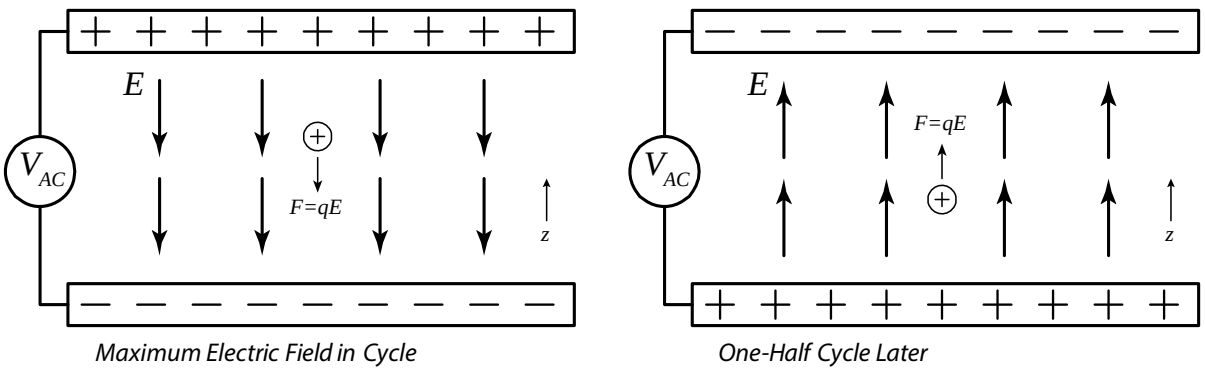

Figure 1. A charged particle placed initially at rest inside a parallel-plate capacitor. An oscillating voltage is applied to the capacitor, so the electric field oscillates with time. At any given time, however, the field is uniform between the plates. The oscillating electric field causes the particle position to oscillate. When the particle position z is high (left), the electric field pushes it down. When the particle z is low (right), the electric field pushes it back up. The average particle position $\langle z \rangle$ remains constant.

To solve this equation, we try a solution of the form $z = A\cos\omega t$, giving

$$\begin{aligned} \dot{z} &= -\omega A \sin\omega t \\ \ddot{z} &= -\omega^2 A \cos\omega t \\ -m\omega^2 A\cos\omega t &= qE_0 \cos\omega t \\ &\Longrightarrow \quad A = -\frac{qE_0}{m\omega^2} \end{aligned}$$

and this gives the full solution

$$z(t) = z_{init} + v_{init}t - \frac{qE_0}{m\omega^2}\cos\omega t \tag{1}$$

where z_{init} is the initial position of the particle and v_{init} is its initial velocity. Note that this solution works in various trivial limits, for example if $q = 0$.

[Note also that you can easily prove to yourself that Equation 1 satisfies the equation of motion – just plug the solution into the equation and see that it works. Proving that Equation 1 is the only possible solution is not so simple. *Uniqueness Theorems* doing just that are the subject of advanced courses in differential equations, and we will not venture into this topic here!]

If we take $v_{init} = 0$, just to make life simpler, then the solution becomes

$$\begin{aligned} z(t) &= z_{init} - \frac{qE_0}{m\omega^2}\cos\omega t \\ &= z_{init} + \Delta z(t) \end{aligned} \tag{2}$$

In other words, the particle stays where we initially placed it (see Figure 1), but the oscillating electric field causes the particle position to oscillate. We will call $\Delta z(t)$ the particle *micromotion*, since we will typically assume this motion is fast and small. Motion over times much longer than $T = 1/\omega$ is often called the *secular* motion.

Note that the particle position is 180 degrees out of phase with the applied force: when Δz is positive, the force is negative, so the force pushes the particle back toward z_{init}. When Δz is negative, the force is positive, so again the force pushes the particle back toward z_{init}. This behavior is shown in Figure 1. So in this simple example the particle just oscillates about z_{init}. If you think about it for a minute, this all makes reasonably good sense.

2.2 Add an Electric Field Gradient

Now we make the problem a bit more interesting by adding a field gradient, so the electric field is no longer uniform

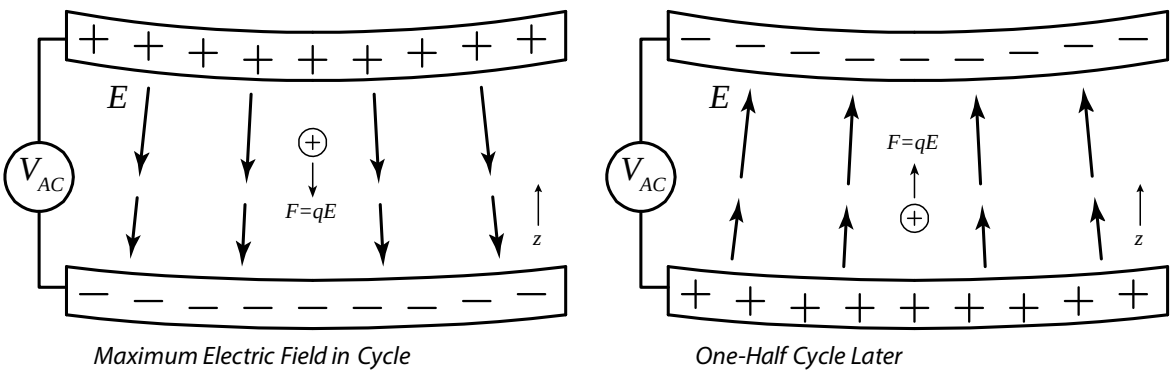

Figure 2. A charged particle placed initially at rest inside a curved-plate capacitor. The geometry of the plates causes a gradient in the electric field strength - the field is stronger for larger z (as shown by the longer arrows) The imbalance means that the electric force on the particle is stronger at the top of its motion (left) and weaker at the bottom (right). Averaging over time, there is a net force that pushes the particle down, toward the weaker-field region.

in space. One way to add an electric field gradient is to curve the plates of our capacitor a bit, as shown in Figure 2. For example, the two plates in the figure might be sections of spherical shells, where the geometrical centers are both located at the same point high above the plates.

The details of the plate geometries are not especially important. What is important is that the electric field lines look roughly like those shown in Figure 2 – in particular, the field strength near the top plate is higher than near the bottom plate (note the lengths of the field vectors in the Figure.) Since we only curved the plates slightly, we haven't changed the field much, so the particle micromotion is about the same as it was before – the particle essentially just oscillates about its initial position.

But now we can see, just from the geometry in Figure 2, that the force over one cycle no longer averages to zero. As shown in the Figure, when Δz is positive (left side of the figure), the particle experiences a stronger-than-average electric field pushing it downward. And when Δz is negative (right side of the figure), the upward force is weaker than average. This imbalance was not present in Figure 1. From this fairly basic reasoning, shown graphically in Figure 2, we deduce that there is a net force pushing the particle down. Put another way, the secular force, averaged over many oscillation cycles, pushes the particle toward a region where the oscillating electric field is weaker.

The math all supports this, as we can demonstrate. We write the modified field as

$$E(z,t) = (E_0 + E'z)\cos\omega t$$

where $E' = dE/dz$. We assume that E' is small, so the particle micromotion is not much different from the $E' = 0$ case. Here we also assume that we are initially placing the particle at $z_{init} = 0$, which is halfway between the plates, just to simplify the equations.

With the added field gradient, the equation of motion becomes

$$m\ddot{z} = q\left(E_0 + E'z\right)\cos\omega t$$

Solving this exactly is nontrivial, but we can capture the essence of the physics by looking at the limit of low E'. Setting $E' = 0$ gives the micromotion we saw previously

$$z(t; E' = 0) = -\frac{qE_0}{m\omega^2}\cos\omega t$$

and for small E' we assume that the micromotion shouldn't change much. We use this to calculate an average force on the particle as follows.

The total force on the particle at any given time is

$$F = q\left(E_0 + E'z\right)\cos\omega t$$

and we write the average force

$$\langle F\rangle = \langle q\left(E_0 + E'z\right)\cos\omega t\rangle$$

where the average is over one oscillation cycle. Since E_0 is constant, we see that

$$\langle qE_0\cos\omega t\rangle = qE_0\left\langle\cos\omega t\right\rangle = 0$$

so

$$\langle F\rangle = \langle qE'z\cos\omega t\rangle$$

Into this we substitute in the $z(t; E' = 0)$ solution to give an approximate answer

$$\begin{aligned}\langle F\rangle &\approx \left\langle qE'\left(-\frac{qE_0}{m\omega^2}\cos\omega t\right)\cos\omega t\right\rangle \\ &\approx -\frac{q^2E'E_0}{m\omega^2}\left\langle\cos^2\omega t\right\rangle\end{aligned}$$

While this is certainly not an exact result, we can expect that it may be reasonably accurate in the limit of low E'. Since $\left\langle\sin^2\omega t\right\rangle = \left\langle\cos^2\omega t\right\rangle$, we can write $\left\langle\cos^2\omega t\right\rangle = \frac{1}{2}\left(\sin^2\omega t + \cos^2\omega t\right) = \frac{1}{2}$, so finally

$$\langle F\rangle \approx -\frac{q^2E'E_0}{2m\omega^2} \tag{3}$$

The negative sign in this expression means that $\langle F\rangle$ pushes the particle toward a region of weaker electric fields. Numerically integrating the equation of motion would give more accurate results, but Equation 3 is a good first step, and it is sufficient for the present discussion. We see that the math confirms our simple reasoning above, and Equation 3 gives a reasonable quantitative approximation for the secular force.

Several key conclusions can be drawn from this discussion: 1) The particle motion separates into two regimes, the *micromotion* that occurs on timescales comparable to the oscillation period, and the *secular motion* that occurs on timescales long compared to the oscillation period; 2) the secular force is reasonably well approximated by Equation 3; and 3) the secular force pushes particles toward regions of weaker oscillating fields.

The last point turns out to be remarkably general, and this is an important fact. For any slowly-varying, physically reasonable field geometry, the secular force always pushes particles toward regions of weaker oscillating fields. We showed this for a special case above; the general case is more difficult to prove, and this is presented in an Appendix below.

One very convenient way to think about all this is with a trap pseudopotential $U_{trap} = (KE)_{micromotion} = \frac{1}{2}mv^2_{micromotion}$. Here the trap pseudopotential U_{trap} is simply equal to the kinetic energy of the particle micromotion. And the secular force is then equal to the gradient of U_{trap}. You can try this in the example above, and you can quickly show that the secular force $\langle F\rangle = dU_{trap}/dz$ is given by Equation 3. A more general derivation of this pseudopotential is given in the Appendix below.

3 Quadrupole Traps

Now that we have a basic understanding of how particles behave in oscillating electric fields, we can proceed to make an ion trap by considering more complex field geometries. We will focus on what are called *quadrupole ion traps*, looking at both 3D and 2D varieties.

One easy way to make a 3D quadrupole trap is shown in Figure 3. An AC voltage is applied to two ball-shaped electrodes in a grounded box, creating oscillatory electric fields inside the box. Halfway between the balls, the electric field is always zero by symmetry. Near this zero-field point, the electric fields at one point in the AC cycle are shown in the Figure. Multiply these vectors by $\cos(\omega t)$ to obtain the electric fields at other times.

With this field geometry we see that the electric field strength increases in all directions outward from the zero-field point halfway between the balls. Thus U_{trap} has a minimum at the zero-field point, since the particle micromo-

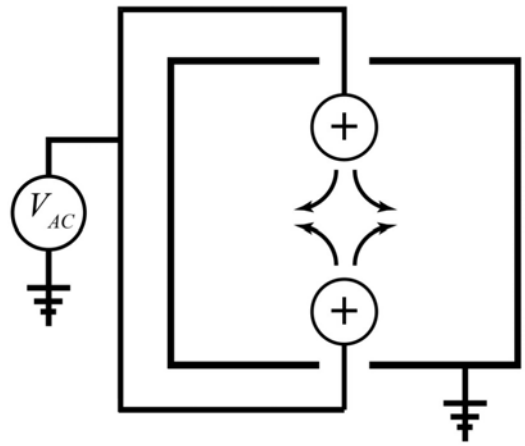

Figure 3. One method for making a 3D quadrupole ion trap, using two ball electrodes in a grounded box. When the balls are at a high potential relative to the box, the electric field lines are shown roughly by the arrows. Note by symmetry the electric field halfway between the balls is always zero.

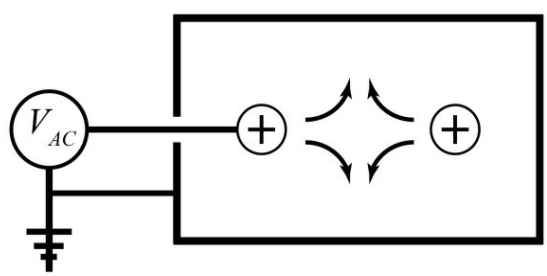

Figure 4. Another method for making a 3D quadrupole trap, which is essentially the geometry used in the Ring Trap, one of three ion traps that are part of the EIT instrument. In this configuration a ring electrode (seen edge-on here) is inside a grounded box, and the potential between the two is set by an applied AC voltage.

tion increases in all directions out from that point. Thus the secular forces will push particles toward the zero-field point, trapping them there.

Another approach for making a 3D quadrupole trap is the Ring Trap shown in Figure 4. Again the electric field at the center of the ring is always zero, and the arrows show the fields in the vicinity of this central region at one point in the cycle.

Both these examples show electric field geometries that: 1) have zero electric field at a center point, 2) have field magnitudes that increase in all directions away from the central point, and 3) exhibit axial symmetry. We can quantify this picture of quadrupole geometries by looking at the fields near the zero-field regions. Around the center points we can do a multipole expansion of the fields, which is essentially a Taylor series expansion of the vector fields (a bit more complicated than a Taylor expansion of a 1D function, but it's the same principle.) Doing this (given without proof here) reveals that the electric potential can be approximated near the trap center $(r = z = 0)$ as

$$V(r,z)_{3D-Quad} = A_0 + A_2\left[2z^2 - r^2\right]\cos\omega t$$

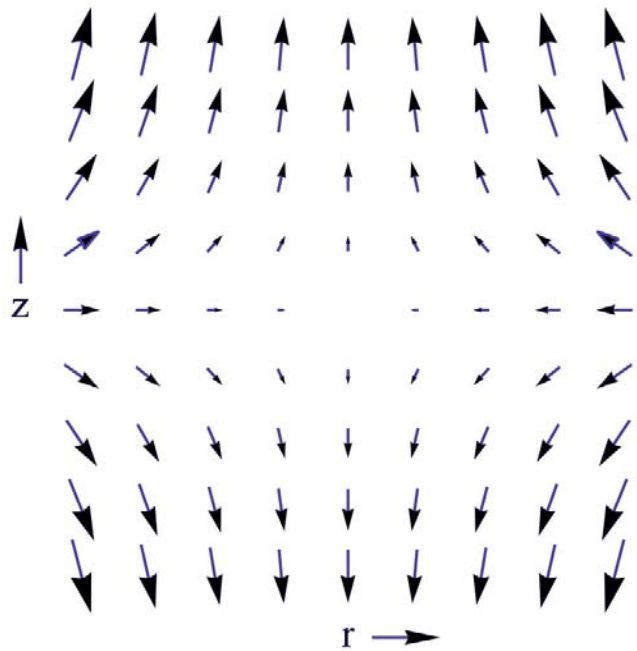

Figure 5. The 3D quadrupolar electric field geometry near the center of the Ring Trap and the Single Particle Trap. This shows the electric field vectors when the ring voltage is at its maximum. Multiply each vector by $\cos(\omega t)$ to obtain the electric fields at other times.

where A_0 and A_2 are constants. The electric fields are then

$$\begin{aligned} E_z &= -\frac{\partial V}{\partial z} = -4A_2 z \cos\omega t \\ E_r &= -\frac{\partial V}{\partial r} = 2A_2 r \cos\omega t \end{aligned} \tag{4}$$

and a vector plot is shown in Figure 5. Note that the electric field strength increases linearly with r and z as one goes out from the origin.

If we do this for the 2D case, then we find (again given without proof here) that the electric potential can be approximated near the trap center $(x = y = 0)$ as

$$V(x,y)_{2D-Quad} = A_0 + A_2\left[x^2 - y^2\right]\cos\omega t$$

where A_0 and A_2 are constants. From this we can calculate the electric fields

$$\begin{aligned} E_x &= -\frac{\partial V}{\partial x} = -2A_2 x \cos\omega t \\ E_y &= -\frac{\partial V}{\partial y} = 2A_2 y \cos\omega t \end{aligned} \tag{5}$$

and a vector plot of these fields is shown in Figure 6. Again we see that the electric field strength increases linearly with x and y near the origin.

At this point it is beneficial to pause, stare at the electric field plots for a while, and ponder what is going on inside these traps. At the trap center, there are no electric fields, so no electric forces at all. A particle at the trap center, with no velocity, would just sit there. Away from the trap center, the electric fields are nonzero, so a charged particle experiences what we are calling the micromotion – it oscillates back and forth, in our case at 60 Hz. Averaging over a few cycles, there is also a weaker secular force that pushes the particles toward the origin. All around the origin, in any direction, the particles are pushed toward the origin. Thus charged particles become trapped at the origin.

Key in this discussion is to separate in your head the micromotion from the secular motion. The micromotion

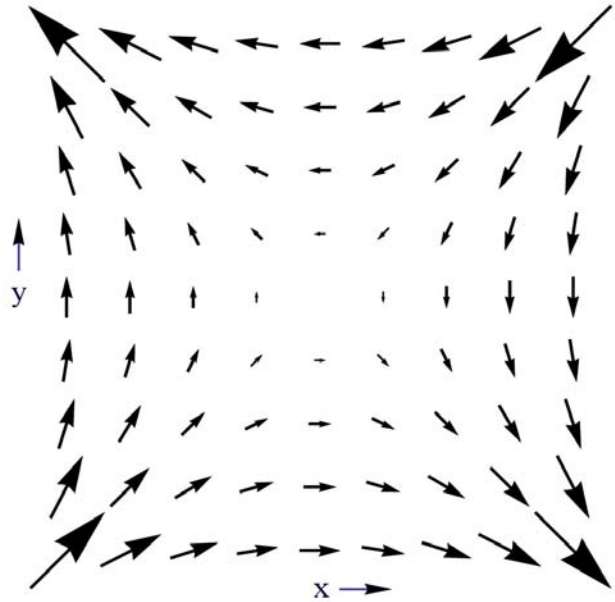

Figure 6. The 2D quadrupolar electric field geometry near the center of the Linear Trap. This shows the electric field vectors when the applied voltage is at its maximum. Multiply each vector by $\cos(\omega t)$ to obtain the electric fields at other times.

exists whenever the oscillating fields are nonzero. But you can average over the micromotion and extract the average secular force $\langle F \rangle$, as we did above. All the stationary forces, such as gravity, combine with $\langle F \rangle$ to determine the long-term behavior of the particle. The pseudopotential U_{trap} is especially useful for visualizing the secular forces.

4 The Triboelectric Series

5 Damped Ion Traps

The above discussion does not include viscous damping from air, which is important. Going back to the parallel-plate capacitor example shown in Figure 1, the electric force remains $F = qE = qE_0 \cos \omega t$, and to this we add viscous damping $F = -\gamma v$, where γ is the usual damping constant and $v = \dot{z}$ is the particle velocity. The equation of motion then becomes

$$\begin{aligned} m\ddot{z} &= qE_0 \cos \omega t - \gamma \dot{z} \\ \ddot{z} + \Gamma \dot{z} &= \frac{qE_0}{m} \cos \omega t \end{aligned}$$

where $\Gamma = \gamma/m$. This time we write the equation in its complex form

$$\ddot{z} + \Gamma \dot{z} = \frac{qE_0}{m} e^{i\omega t}$$

solution of the form $z = Ae^{i\omega t}$, giving

$$\begin{aligned} -\omega^2 A e^{i\omega t} + i\omega\Gamma A e^{i\omega t} &= \frac{qE_0}{m} e^{i\omega t} \\ A &= -\frac{qE_0/m}{\omega^2 - i\omega\Gamma} \end{aligned}$$

Table 1. The Triboelectric Series

Most Positive (+)	
Air	
Human Hands, Skin	
Asbestos	
Rabbit Fur	+++
Glass	
Human Hair	
Mica	
Nylon	
Wool	
Lead	
Cat Fur	+
Silk	
Aluminum	
Paper	
Cotton	
Steel	
Wood	
Lucite	
Sealing Wax	-
Amber	
Rubber Balloon	
Hard Rubber	
Mylar	
Nickel	
Copper	
Silver	
uv Resist	
Brass	
Synthetic Rubber	
Gold, Platinum	
Sulfur	
Acetate, Rayon	
Polyester	
Celluloid	
Polystyrene	
Orlon, Acrylic	
Cellophane Tape	
Polyvinylidene chloride (Saran)	
Polyurethane	
Polyethylene	
Polypropylene	
Polyvinylchloride (Vinyl)	
Kel-F (PCTFE)	- - -
Silicon	
Teflon	
Silicone Rubber	
Most Negative (-)	

Figure 7. A diagram showing the Triboelectric Series, adapted from http://www.siliconfareast.com/tribo_series.htm. Materials near the top tend to become positively charged when rubbed, while those near the bottom become negatively charged. In the Electrodynamic Ion Traps apparatus we use Teflon and Nylon “wands” to pick up, charge, and deliver particles for trapping.

and the final solution (assuming $v_{init} = 0$) is given by the real part of the complex solution, giving

$$\begin{aligned} z(t) &= z_{init} - \mathrm{Re}\left[\frac{qE_0/m}{\omega^2 - i\omega\Gamma} e^{i\omega t}\right] \\ &= z_{init} + \Delta z(t) \end{aligned}$$

Note that if we assume $\Gamma = 0$ (no damping), then we recover the solution above, in Equation 2. If $\Gamma > 0$, then note that the amplitude of the oscillatory term is always smaller than what we found above. This makes sense; we would expect the addition of damping to reduce the amplitude of driven oscillations.

Carrying the math a bit further, we have

$$\begin{aligned} \Delta z(t) &= -\mathrm{Re}\left[\frac{qE_0/m}{\omega^2 - i\omega\Gamma} e^{i\omega t}\right] \\ &= -\mathrm{Re}\left[\frac{qE_0/m}{\omega^2 - i\omega\Gamma}\frac{\omega^2 + i\omega\Gamma}{\omega^2 + i\omega\Gamma} e^{i\omega t}\right] \\ &= -\frac{qE_0/m}{\omega^4 + \omega^2\Gamma^2}\,\mathrm{Re}\left[\left(\omega^2 + i\omega\Gamma\right)\left(\cos\omega t + i\sin\omega t\right)\right] \\ &= -\frac{qE_0}{m}\frac{1}{\omega^4 + \omega^2\Gamma^2}\left[\omega^2\cos\omega t - \omega\Gamma\sin\omega t\right] \\ &= -\frac{qE_0}{m}\frac{1}{\omega^2 + \Gamma^2}\left[\cos\omega t - \frac{\Gamma}{\omega}\sin\omega t\right] \end{aligned}$$

And again we note that this reduces to Equation 2 when $\Gamma = 0$, as we would expect.

We now compute the trapping force by averaging over one cycle, as we did above. The force on the particle at any given time is

$$F = q\left(E_0 + E'z\right)\cos\omega t$$

and the average force becomes (see above)

$$\begin{aligned} \langle F\rangle &= \langle qE'z\cos\omega t\rangle \\ &\approx \left\langle qE'\left(-\frac{qE_0}{m}\frac{1}{\omega^2 + \Gamma^2}\left[\cos\omega t - \frac{\Gamma}{\omega}\sin\omega t\right]\right)\cos\omega t\right\rangle \end{aligned}$$

Since $\langle\sin\omega t\cos\omega t\rangle = 0$, this becomes

$$\begin{aligned} \langle F\rangle &\approx \left\langle qE'\left(-\frac{qE_0}{m}\frac{1}{\omega^2 + \Gamma^2}\cos\omega t\right)\cos\omega t\right\rangle \qquad (6) \\ &\approx -\frac{q^2E'E_0}{m}\frac{1}{\omega^2 + \Gamma^2}\left\langle\cos^2\omega t\right\rangle \\ &\approx -\frac{q^2E'E_0}{2m}\frac{1}{\omega^2 + \Gamma^2} \end{aligned}$$

Comparing this with Equation 3, we see that damping reduces $\langle F\rangle$ compared to the $\Gamma = 0$ case, which again seems intuitively plausible.

5.1 Stokes Damping

To calculate the damping constant, we start with the Reynolds number

$$R_e \approx \frac{\rho v R}{\mu}$$

where ρ is the fluid density, v is the particle velocity, R is the particle radius, and μ is the dynamical viscosity. For our trapped particles in air, $v \approx 1$ mm/(1/60 sec) ≈ 6 cm/sec, $R \approx 10$ μm, and for air at a pressure of one atmosphere we have $\rho \approx 1.2$ kg/m^3 and

$$\mu = 1.8 \times 10^{-5}\ \frac{\text{kg}}{\text{m-s}}$$

so $R_e \approx 0.04$.

For such a low Reynolds number, the air damping is well approximated by Stokes damping, given by

$$F = -6\pi\mu R v$$

and we see that the force is proportional to $-v$, which is typical of a friction force. This gives a damping constant

$$\gamma = 6\pi\mu R$$

and

$$\begin{aligned}\Gamma &= \frac{\gamma}{m} \\ &= \frac{6\pi\mu R}{\frac{4}{3}\pi R^3 \rho_{part}} \\ &= \frac{9}{2}\frac{\mu}{R^2\rho_{part}}\end{aligned}$$

where ρ_{part} is the particle density.

Assuming a density of $\rho_{part} \approx 500$ kg/m^3, and using the other parameters above, this gives

$$\Gamma \approx 1620 \text{ s}^{-1}$$

which is substantially larger than $\omega = 2\pi(60 \text{ Hz}) = 377 \text{ s}^{-1}$. For example, the secular trapping force in Equation 6 becomes

$$\langle F \rangle \approx -\frac{q^2 E' E_0}{2m\Gamma^2}$$

to an accuracy of about five percent.

With this "overdamped" approximation, the micromotion becomes

$$\begin{aligned}E(t) &= E_0 \cos\omega t \\ \Delta z(t) &= -\operatorname{Re}\left[\frac{qE_0/m}{\omega^2 - i\omega\Gamma} e^{i\omega t}\right] \\ &\approx \operatorname{Re}\left[\frac{qE_0/m}{i\omega\Gamma} e^{i\omega t}\right] \\ &\approx \frac{qE_0}{m\omega\Gamma}\sin\omega t\end{aligned}$$

In the overdamped limit, the motion is 90 degrees out of phase with the drive force, rather than 180 degrees out of phase, as we saw above.

5.2 Particle Dynamics in a Quadrupole Trap

Next consider a particle in a 3D quadrupole trap, and look at the motion. From Equation 4, the oscillatory electric field is

$$\begin{aligned}E_z &= -4A_2 z \cos\omega t \\ &= E_0(z)\cos\omega t\end{aligned}$$

so $E_0(z) = -4A_2 z$, where A_2 depends on the applied voltage and the geometry of the trap. For convenience we can write

$$E_0(z) = \frac{V_{AC}}{z_{eff}^2} z$$

where z_{eff} is a constant that depends on the geometry of the trap, and we expect z_{eff} to be comparable to the spacing between the trap electrodes. This replaces one constant (A_2) with another, more physically defined, constant (z_{eff}). We are also free to define the sign of V_{AC} to remove the minus sign from the expression. Changing the constants in this way simply makes the subsequent math a bit simpler and more intuitive.

The field gradient is

$$\begin{aligned} E'(z) &= \frac{dE_0(z)}{dz} \\ &= \frac{V_{AC}}{z_{eff}^2} \end{aligned}$$

The trapping force is then

$$\begin{aligned} \langle F \rangle &\approx -\frac{q^2 E' E_0}{2m} \frac{1}{\omega^2 + \Gamma^2} \\ &\quad -\frac{q^2}{2m} \left(\frac{V_{AC}}{z_{eff}^2} \right)^2 \frac{1}{\omega^2 + \Gamma^2} z \\ &\approx -\frac{q^2 V_{AC}^2}{2m z_{eff}^4} \frac{1}{\omega^2 + \Gamma^2} z \\ &\approx -\frac{q^2 V_{AC}^2}{2m z_{eff}^4 \Gamma^2} z \end{aligned}$$

using overdamped approximation, which is accurate to about 4 percent.

Apply an external force F_{ext}, then the particle will settle to an equilibrium position z_{eq} where the trapping force $\langle F \rangle$ balances the external force F_{ext}, giving

$$\begin{aligned} \frac{q^2 V_{AC}^2}{2m z_{eff}^4 \Gamma^2} z_{eq} &\approx F_{ext} \\ z_{eq} &\approx \frac{2m z_{eff}^4 \Gamma^2}{q^2 V_{AC}^2} F_{ext} \end{aligned}$$

If we let $F_{ext} = qE_{static} - mg$, then

$$\begin{aligned} z_{eq} &\approx \frac{2m z_{eff}^4 \Gamma^2}{q^2 V_{AC}^2} (qE_{static} - mg) \\ &\approx \frac{2m z_{eff}^4 \Gamma^2}{q V_{AC}^2} \Delta E_{static} \end{aligned}$$

where

$$\Delta E_{static} = E_{static} - \frac{mg}{q}$$

Balancing gravity gives us a measurement of q/m, and z_{eff} is derived from the trap geometry. Thus a measurement of the slope of $z_{eff}(\Delta E_{static})$ gives direct measure of Γ, and from this the particle radius R can be independently determined.

Also measure micromotion under application of ΔE_{static}

$$\Delta z(t) = -\frac{qE_0}{m} \frac{1}{\omega^2 + \Gamma^2} \left[\cos \omega t - \frac{\Gamma}{\omega} \sin \omega t \right]$$

Amplitude of oscillation in overdamped approximation ($\Gamma \gg \omega$)

$$\begin{aligned} \Delta z_{\max} &\approx \frac{qE_0}{m} \frac{1}{\omega^2 + \Gamma^2} \frac{\Gamma}{\omega} \\ &\approx \frac{qE_0}{m} \frac{1}{\omega \Gamma} \\ &\approx \frac{q}{m} \frac{1}{\omega \Gamma} \frac{V_{AC}}{z_{eff}^2} z_{eq} \\ &\approx \frac{q}{m} \frac{1}{\omega \Gamma} \frac{V_{AC}}{z_{eff}^2} \frac{2m z_{eff}^4 \Gamma^2}{q V_{AC}^2} \Delta E_{static} \\ &\approx \frac{2 z_{eff}^2 \Gamma}{\omega V_{AC}} \Delta E_{static} \end{aligned}$$

so again measure Γ.

Unstable orbit when $\Delta z_{\max} = z_{eq}$, which from the above means

$$\frac{q}{m}\frac{1}{\omega\Gamma}\frac{V_{AC}}{z_{eff}^2} = 1$$

so stability requires

$$V_{AC} < \frac{m\omega\Gamma z_{eff}^2}{q}$$

and once again we measure Γ.

6 Extended Orbits

When the AC fields are turned up in the EIT apparatus, one often sees extended particle orbits. These are particularly apparent in the Linear Trap and in the Single Particle Trap. Explaining these orbits is a fairly advanced topic, and a full description of the phenomenon requires numerical modeling of the particle dynamics. What follows is not a complete treatment, but rather a fairly qualitative description of the phenomenon.

6.1 The Ring Trap

First consider the 3D quadrupole electric field geometry near the center of the Ring Trap, which is the same as that near the center of the Single Particle Trap, as was shown above in Figure 5. Put a particle in the trap, with a downward static force provided by gravity. Since the motion of the particle is overdamped, its micromotion velocity is nearly proportional to the applied electric field. (Put another way, the particle motion is overdamped, so the particle velocity is always roughly equal to the terminal velocity resulting from the electric and gravitational forces.) In this overdamped approximation, Figure 8 shows the particle position and velocity as a function of time. For this particle we have that: 1) the particle is displaced downward from gravity, so its mean position is below the trap center; 2) the secular trapping force $\langle F \rangle$ is directed upward, toward the trap center, and this time-averaged force equals the downward gravitational force, so $\langle z \rangle$ is constant; 3) at this $\langle z \rangle$, the particle exhibits micromotion caused by the oscillating fields, which is the source of the trapping force; and 4) this is a stable oscillating state of the particle.

If we slowly increase the applied AC voltage to the trap, at first the particle motion will remain about the same as that shown in Figure 8. However the highest z position reached by the particle will become closer to the trap center. At some point this highest z position will equal and then go above the trap center, and at this point the motion will transition into an extended orbit, as shown in Figure 9. Note that in Figure 8 the particle completed one cycle in a time P, while in Figure 9 it takes $2P$ to complete the full extended orbit.

Figure 10 shows measurements of an extended orbit, for a particle held in the Single Particle Trap. A full analysis of these data would require a numerical analysis, but one can see the essential features described in Figure 9. We see, for example, that at $t \approx 14$ msec the particle overshot, crossing above the trap center, and we can infer that at $t \approx 16$ msec the electric field amplitude went through zero, and at this time the particle velocity was low. Note also that the electric fields are always low near the trap center, so things happen more slowly there. The fields away from the trap center are stronger, however, and this explains why the reversal at $t \approx 25$ msec was especially rapid. Figure 10 also shows that the whole process repeated as the particle oscillated between positive z and negative z, taking 1/30th second for a full orbit.

These extended orbits are commonly seen in the Ring Trap and in the Single Particle Trap, and we see from the discussion above that basic mechanics readily explains the underlying dynamics at a qualitative level. Even without sophisticated mathematical analysis or lengthy numerical simulations, one can understand the fundamental physics that produces these extended orbits.

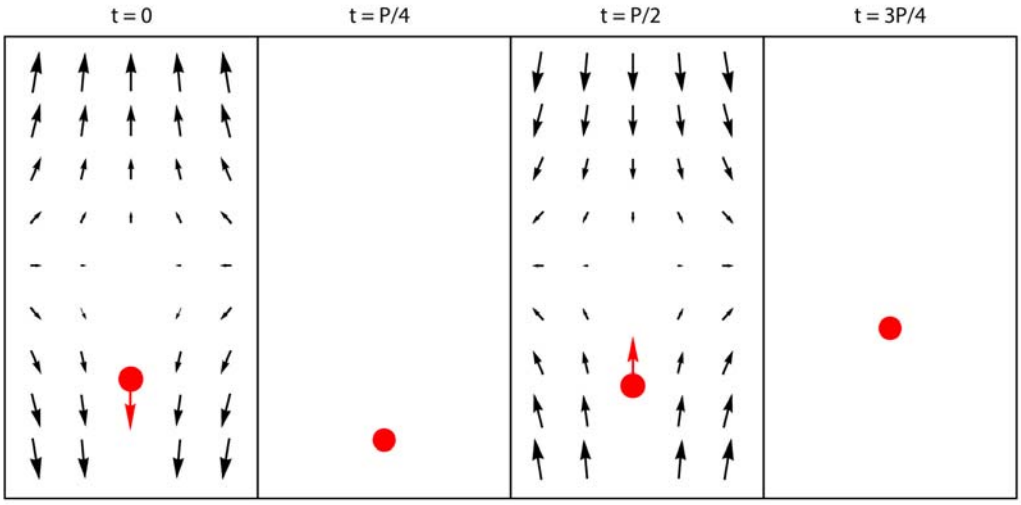

Figure 8. The micromotion of a trapped particle in a 3D quadrupole trap (e.g. the Ring Trap or the Single Particle Trap), where gravity displaces the particle down from the trap center. (Note that some electric field vectors in the particle path are not shown, for clarity.) In panel 1, the electric fields pulls the particle down. Since the particle motion is strongly damped, the particle velocity is roughly proportional to the electric field strength. In panel 2, a quarter cycle later, there is zero electric field (so no field vectors in this panel) and the particle motion is quickly damped away. In panel 3, the electric field pulls the particle up again. And in panel 4, the field and the particle velocity again go to zero. The time-averaged (secular) trapping force is upward, balancing the downward pull of gravity. Thus the oscillatory vertical motion of the particle is stable, repeating in time with a period P.

6.2 The Linear Trap

Extended orbits of a different nature are seen in the Linear Trap, as shown in Figure 11. These extended orbits are commonly seen in the Linear Trap, and their explanation is similar to that above. We begin with the 2D quadrupolar electric field geometry shown in Figure 12, which results in the stable orbit shown. This micromotion is analogous to that shown in Figure 8. The geometry is different for the Linear Trap, but the underlying dynamics is similar for the 2D and 3D cases.

As the trapping voltage is turned up, the micromotion shown in Figure 12 at first remains essentially unchanged, except the endpoints of the motion move closer to the diagonal lines connecting the corners of the trap. As long as the endpoints do not cross those lines, then the particle remains confined to the lower quadrant, as shown in Figure 12.

As the trapping voltage is increased above some threshold, however, then the particle motion will transition into an extended orbit, as shown in Figure 13. In the 3D quadrupole case above, this happened with the micromotion carried the particle above the trap center. In the 2D case shown in Figure 12, the transition occurs when the micromotion overshoots the diagonals connecting the corners of the trap. Then the particle is no longer confined to the lower quadrant, and it begins executing an extended orbit, and again the extended orbit has double the period of the simple orbit. Although the geometries of the extended orbits in the two cases above are different, the underlying physics is quite similar.

Figure 14 shows examples of the simple and extended orbits in the Linear Trap. (Note that an additional mirror, not provided with the EIT instrument, is needed to view these orbits face-on in this way.) We have observed that the simple orbits in the Linear Trap are quite stable, but the elongated orbits exhibit a rich behavior, as demonstrated in Figure 15. These orbits are easily perturbed and quite fascinating to watch, and it appears likely that there may chaotic regimes in the trap parameter space.

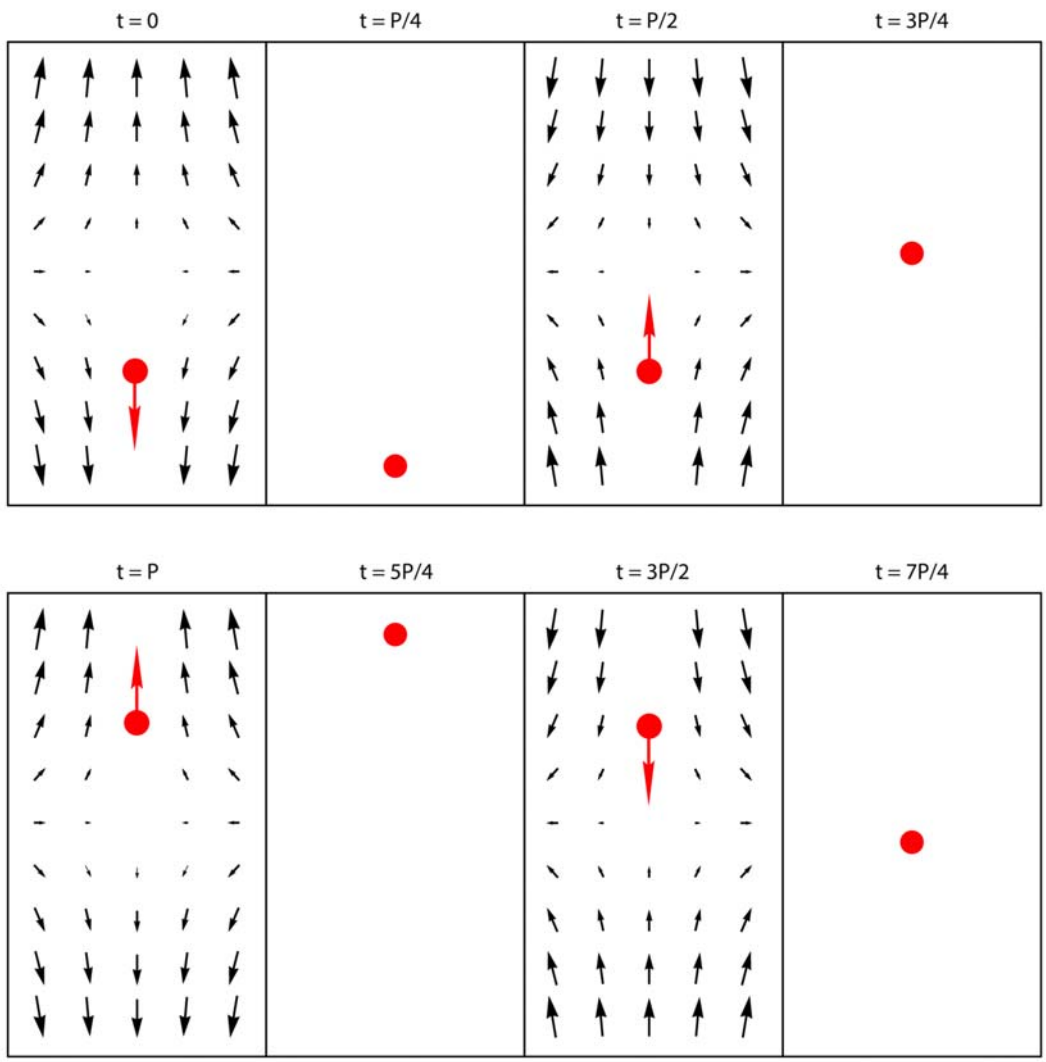

Figure 9. A particle in a 3D quadrupolar field exhibiting an extended orbit. In the top four panels in this Figure, we see that the particle motion is similar to that described in Figure 8, except this time the particle overshoots above the center of the trap. When the field increases again (the fifth panel), the particle is then pushed up, taking it farther above the trap center. When it comes back down, it again overshoots beyond the trap center, so the fields push it into the lower half of the trap again. A complete cycle thus takes time $2P$, whereas a time P was needed for the simpler orbit in Figure 8.

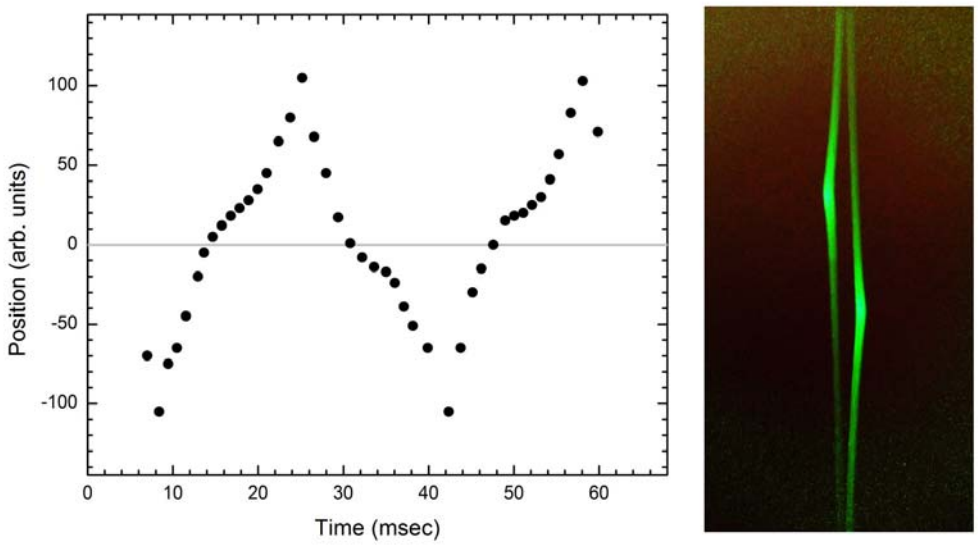

Figure 10. The graph on the left shows the measured position z of a particle in the Single Particl Trap (where z is measured relative to the trap center) as a function of time, as the particle executed an extended orbit. These data were obtained by analyzing a video taken when the laser was strobed. The image on the right shows a longer exposure, zoomed in on the center of the trap. The brighter regions show where the particle slowed during its orbit.

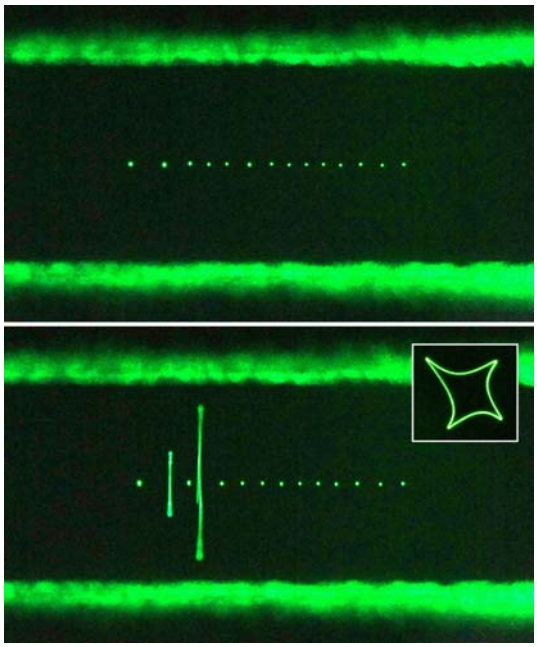

Figure 11. Two photographs of particles held in the Linear Trap. The top image shows a line of ions in a stable Coulomb crystal. When the AC voltage is turned up above a threshold, some of the particles transition into extended orbits, and these orbits are seen edge-on in the lower image. The inset shows one such extended orbit in a face-on view.

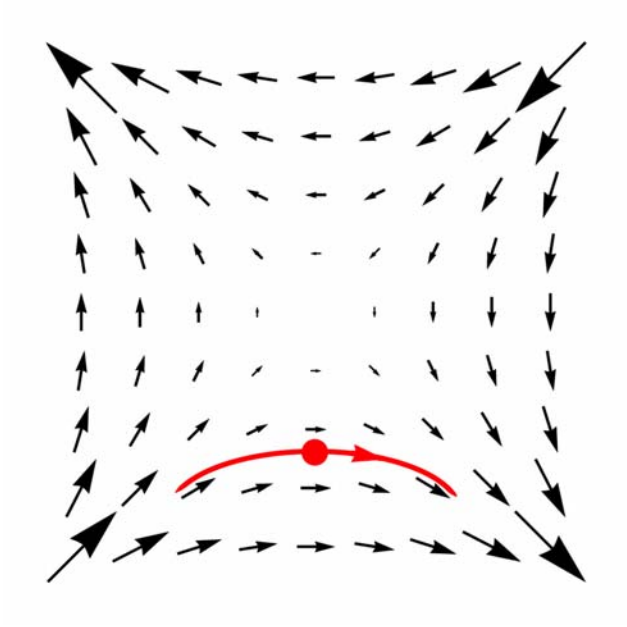

Figure 12. The 2D quadrupolar electric field geometry near the center of the Linear Trap. At this phase of the cycle, the electric fields push the particle (red) to the right (red arrow). As the cycle progresses, the particle is pushed back and forth, executing the orbit shown by the red line. This stable orbit has a period P, and it is the analog of the stable orbit shown in Figure 8. As in that Figure, we are assuming that gravity is displacing the particle down from the trap center. Note that the particle motion is confined to the lower quadrant of the trap, the quadrants being defined by diagonal lines connecting the corners of the trap.

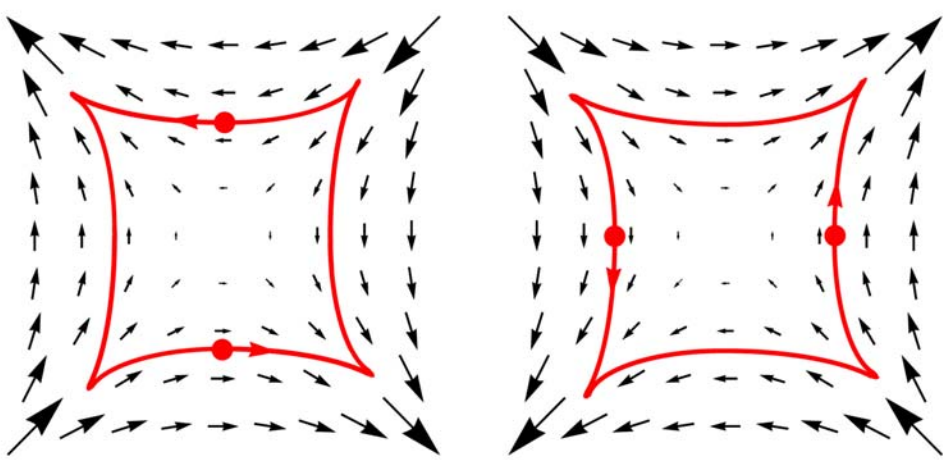

Figure 13. An extended particle orbit in the Linear Trap. Here the electric fields are strong enough to cause the particle to overshoot the diagonals, and when this happens the motion is no longer confined to the lower quadrant. The particle executes the extended orbit shown, and the time required for a complete orbit is $2P$.

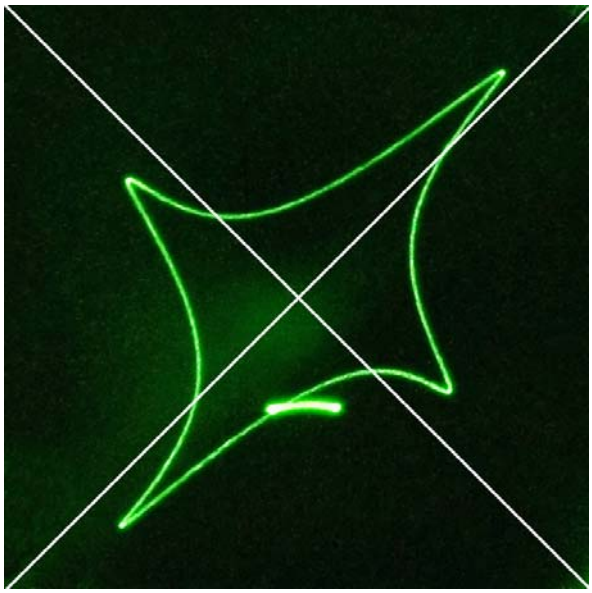

Figure 14. Examples of simple and extended orbits in the 2D quadrupolar geometry. This photograph was taken from along the axis of the Linear Trap, and it shows two particles simultaneously trapped. The short streak in the lower quadrant came from a particle in a simple orbit. The larger line shows a particle in an extended orbit. Note that one can infer from this orbit that the particle was traveling counterclockwise. The exposure for this photograph was greater than 1/30th second, and the diagonal lines were added digitally to define the quadrants.

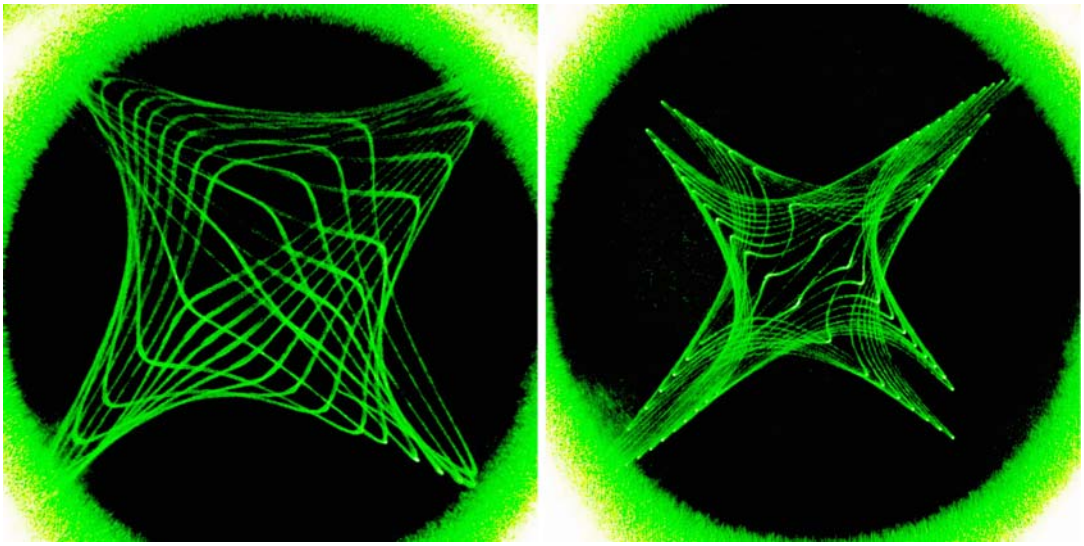

Figure 15. The extended orbits seen in the Linear Trap exhibit quite a variety of surprising behaviors. These photographs had exposure times of roughly a dozen orbits, and they illustrate how the orbits can evolve in complex ways over short times.